Definition of Contingency Criticality Based on Violation Probability of Voltage Security Margin Considering Correlated Uncertainties in System Loads and Wind Power Generation

Gustavo Gonçalves dos Santos, Matheus Rosa Nascimento, *Member*, *IEEE*, João Pedro Peters Barbosa, *Member*, *IEEE*, Maiara Camila Oliveira, Ahda Pionkoski Grilo Pavani, *Senior Member*, *IEEE*, and Rodrigo Andrade Ramos, *Senior Member*, *IEEE*

***Abstract*—The massive integration of intermittent renewable generation and the increasing variability of demand raise concerns about the high level of uncertainty in the security assessment of power systems. In this context, the main contribution of this study is the proposal of a new definition of contingency criticality, which is based on the violation probability of the voltage security margin (VSM) while considering correlated uncertainties in both system loads and wind power generation. From this new definition, a contingency ranking can be derived and used to determine preventive control actions. To calculate this probability for each contingency, a new approach based on the cross-entropy (CE) method is developed and applied. The CE method is well-suited to handle high levels of uncertainty, as it typically provides faster and more accurate results compared with Monte Carlo simulation, particularly for cases with low violation probabilities of the VSM. Another innovative feature of this approach is the consideration of correlated uncertainties through the use of multivariate normal distributions and Gaussian copulas. Furthermore, the proposed definition is implemented using a formulation that is capable of detecting either saddle-node or limit-induced bifurcations to accurately identify the maximum loadability point. A proof of concept is presented for a comprehensive explanation of the proposed definition, followed by an application of this definition to the IEEE 118-bus test system. The findings of this paper highlight the need to carefully select critical contingencies for voltage security assessment in the context of increasing uncertainties.**

***Index Terms*—Critical contingency, violation probability, uncertainty, wind power, limit-induced bifurcation, cross-entropy method, probabilistic stability assessment, voltage security margin, voltage stability.**

I. Introduction

THE decarbonization goals set by several countries around the world often conflict with the rapid and diverse growth in power consumption. This issue is reflected in many types of power system studies, including stability and dynamic security assessments [1]. For example, the Brazilian National System Operator reported a record-high aggregate load of its interconnected system, surpassing 100 GW of peak demand. This high loading of the system was associated with a significant temperature increase observed across much of the country [2]. These extreme climate events are expected to become increasingly frequent, which highlights the need to quantify and manage the risk of voltage instability due to their relation to high load levels [1].

In its broadest sense, voltage stability refers to the ability of a power system to maintain steady voltages at all buses in the system after being subjected to a disturbance [3]. There is a class of methods for voltage stability analyses that employs static approaches, which are applicable to long-term studies of subsequent equilibria caused by a slow and sustained load buildup. Starting from a base case and following a predefined load growth direction, the objective of these studies is to calculate the maximum additional amount of aggregate active power that can flow across the transmission system (known as voltage stability margin [4]). However, for safety reasons, transmission system operators usually define an upper limit on the allowable increase in the aggregate active power, which must be smaller than the voltage stability margin. This upper limit is then used to define the voltage security margin (VSM) [5] of the system under the previously described conditions.

Manuscript received: September 28, 2024; revised: February 10, 2025; accepted: April 21, 2025. Date of CrossCheck: April 21, 2025. Date of online publication: May 23, 2025.

This work was partly supported by the São Paulo Research Foundation (FAPESP) under Grants 2018/20104-9 and 2023/09332-8. We gratefully acknowledge the support of the RCGI – Research Centre for Greenhouse Gas Innovation (23.1.8493.1.9), hosted by the University of São Paulo (USP), sponsored by FAPESP (2020/15230-5), and sponsored by TotalEnergies, and the strategic importance of the support given by ANP (Brazil's National Oil, Natural Gas and Biofuels Agency) through the R&DI levy regulation. We also acknowledge the support for R&D from TotalEnergies EP Brasil through financing the project "Mitigate curtailment of renewable generation with optimal allocation of energy resources and FACTS in Brazilian Power System" (ANP code 23655-4).

G. G. dos Santos, M. R. Nascimento, J. P. P. Barbosa, M. C. Oliveira, and R. A. Ramos (corresponding author) are with the São Carlos School of Engineering, University of São Paulo, São Carlos, Brazil (e-mail: g.gustavo.santos@usp.br; rmatheus@usp.br; jpeters@usp.br; maiaracoliveira@usp.br; rramos@usp.br).

A. P. G. Pavani is with the Center for Engineering and Applied Social Sciences of the Federal University of ABC, Santo André, Brazil (e-mail: ahda.pavani@ufabc.edu.br).

DOI: 10.35833/MPCE.2024.001077

System operators around the world rely mostly on variations of the continuation power flow (CPF) [6] to estimate the VSM. However, in contingency analyses, the use of these variants (such as the one in [7]) may involve an excessively high computational burden due to the increasing uncertainties in the load growth patterns and generation redispatch rules introduced by new decarbonization-related technologies. Indeed, the consideration of uncertainties in voltage stability assessment has been a focus of attention of the power system community recently [8]-[10].

Efficient approaches to calculating the VSM (such as the one in [11]) can be excessively conservative since their goal is to determine the worst-case scenario with no discussion on the likelihood of its occurrence. More useful information for system operators is the probability of occurrence of a small VSM, which is directly related to the risk of voltage instability. A stochastic voltage stability assessment employing the Monte Carlo simulation (MCS) method offers a straightforward way to account for various uncertainties, but the heavy computational burden renders this method unattractive and impractical, posing a significant challenge in the context of large-scale networks. Recent publications have explored alternative sampling techniques to either substitute or accelerate the MCS method to solve VSM problems.

In [12], the stochastic response surface method was used to establish surrogate models of load margins. This method models the response of the system using polynomial chaos expansion with standard random variables, and the resulting probability distributions significantly reduce the computational burden of the method when compared with the MCS method. However, estimating the coefficients of the polynomial expansion is challenging, particularly for large systems with many uncertainties. The surrogate model may also be ineffective in dealing with topology changes (such as contingencies). To address this issue, a neural network is used to improve the surrogate model in [13]. The success of this approach largely depends on the availability of a suitable training dataset, which can be a practical constraint for most of its applications.

The Latin hypercube sampling (LHS) was used in [14] as another approach to reduce the computational burden of MCS method. However, for large systems with many uncertain inputs, the combination with other techniques (such as Nataf transformation, *K*-means clustering, and maximum entropy model) may require a computational cost comparable to the MCS method.

Considering all possible operating scenarios, those with small VSM are rare instances. Therefore, in a probabilistic framework, importance-sampling techniques are recommended to handle such problems. The cross-entropy (CE) method has been widely used to enhance the efficiency of MCS method in estimating rare events in power systems [15]-[18]. In the context of voltage stability, [17] (which estimates the worst-case scenario) and [18] (which groups critical scenarios) employed the CE method to identify conditions with small VSM. Neither work calculated the probability of occurrence of these VSMs, which is a drawback because critical margins with a near-zero probability of occurrence may be excessively conservative for operation planning.

This work employs a probabilistic approach to voltage security analysis, rather than a deterministic one based on a worst-case scenario such as those adopted by [18] and [19]. Instead of the base or worst-case scenarios, operating points characterized by $N-1$ contingencies are investigated in this paper, as opposed to [12], [14], [20]-[23], in which scenarios with network topology changes are not considered. Analyzing topology changes is fundamental for voltage stability assessment, given that the system almost always becomes more vulnerable under contingencies. If contingency criticality is related to the violation of the VSM, contingencies classified as non-critical when evaluated at base case may become critical due to uncertainties under this operating condition.

Therefore, this paper presents a unique methodology for the definition of contingency criticality. This new definition is the main and most important contribution of this paper, and it becomes increasingly relevant as the degree of uncertainty in the operation of the system grows. The proposed methodology, based on a variant of the CE method, is suitable for estimating violation probabilities of VSMs even if they are rare events (which might jeopardize estimation by methods such as LHS). Moreover, in this work, VSMs are calculated based on a Jacobian matrix expansion, making it possible to detect both limit-induced bifurcation (LIB) and saddle-node bifurcation (SNB). Previous studies on LIB detection, such as [24]-[26], can be considered as CPF variants and did not test their method performance for systems with load and generation uncertainties.

To highlight the contributions of this paper, a summary of them is given below in order of relevance and novelty.

1) The paper proposes a new definition of contingency criticality. It is based on the violation probability of the VSM, taking into account uncertainties in both the system loads and the wind power generation.

2) Based on the calculated probabilities, the proposed definition ranks the criticality of the contingencies in decreasing order, in such a way that the resulting list is compliant with grid codes.

3) A new approach based on the CE method is developed to efficiently and accurately calculate these probabilities.

4) This new approach innovates by considering correlated uncertainties with the use of multivariate normal distributions and Gaussian copulas.

5) Another novelty of this new approach is the use of a formulation capable of detecting both SNB and LIB to accurately detect the maximum loadability point.

The remainder of this paper is structured as follows: Section II provides the mathematical formulation proposed for the calculation of VSMs. Section III describes the foundations for the models of uncertainties in load and intermittent generation, as well as the proposed approach based on the CE method to calculate the violation probability of the VSM. Section IV presents the proposed definition of the contingency criticality. Section V shows numerical results to comprehensively explain and demonstrate the applicability of the proposed approach. Section VI outlines the conclu-

sions.

II. Mathematical Formulation Proposed for Calculation of VSMs

For long-term voltage stability analyses, an electric power system can be modeled (considering a load growth direction) as:

$$\boldsymbol{f}(\boldsymbol{z},\lambda)=\boldsymbol{0} \quad \boldsymbol{z}\in\mathbb{R}^n,\lambda\in\mathbb{R} \tag{1}$$

where $\boldsymbol{z}$ is the system state vector; λ is a parameter associated with active load growth [18]; and $\boldsymbol{f}(\cdot)$ is a multivariate function defined in [27]. This system model reaches its maximum loadability at $\lambda=\lambda_*$, which characterizes a bifurcation point.

In this paper, the direct method described in the following is used to compute λ_*, which enables the calculation of the VSM.

A. Mathematical Model for Load Growth Direction

For simplicity, a constant power model is employed to describe the load. This type of model is commonly employed in long-term voltage stability analyses since it produces conservative estimates of the VSM [28]. The apparent power of all loads is assumed to grow as a function of the parameter λ with a constant power factor. Thus, the growth of the demanded active power starting from the current operating point can be represented by $\boldsymbol{P}_L$ and calculated as:

$$\boldsymbol{P}_L=\boldsymbol{P}_{L0}+\lambda\boldsymbol{b}_{PL} \tag{2}$$

where $\boldsymbol{b}_{PL}\in\mathbb{R}^{N_L}$ is the vector of growth directions of N_L loads; and $\boldsymbol{P}_{L0}$ is the aggregate of the demanded active power at the current operating point.

This load growth requires the redispatch of non-intermittent generation. The aggregate power output of the non-intermittent generators $\boldsymbol{P}_G$ is defined by using (3a), in which b_{PLi} is the component of $\boldsymbol{b}_{PL}$. Intermittent generation units (such as wind farms) are represented as power injections modeled by stochastic variables, so they are not considered in (3a). Only synchronous generators are redispatched, so $\boldsymbol{P}_{G0}$ is defined in such a way that $\boldsymbol{P}_{G0}-\boldsymbol{P}_{L0}$ corresponds to the aggregate power output of non-intermittent generators.

$$\boldsymbol{P}_G=\boldsymbol{P}_{G0}+\boldsymbol{\alpha}\sum_{i=1}^{N_L}\lambda b_{PLi} \tag{3a}$$

$$\alpha_i=\frac{P_{Gi\max}-P_{Gi0}}{\sum_{j=1}^{N_G}(P_{Gj\max}-P_{Gj0})} \tag{3b}$$

where $\boldsymbol{\alpha}=[\alpha_1,\alpha_2,\ldots,\alpha_i,\ldots,\alpha_{N_G}]$ is the vector of participation factors of N_G synchronous generators according to the rule given by (3b), subjected to $\sum\alpha_i=1$; and P_{Gi0} and $P_{Gi\max}$ are the base case and maximum active power outputs of the i^{th} synchronous generator, respectively.

B. Direct Method Based on an Expanded Jacobian Formulation

According to [27], an SNB point, which is characterized by the steady-state Jacobian $\partial\boldsymbol{f}/\partial\boldsymbol{z}$ with a single zero eigenvalue, can be calculated using the following set of equations:

$$\boldsymbol{f}(\boldsymbol{z}_*,\lambda_*)=\boldsymbol{0} \tag{4a}$$

$$\boldsymbol{w}^{\mathrm{T}}\frac{\partial\boldsymbol{f}}{\partial\boldsymbol{z}}\Big|_{(\boldsymbol{z}_*,\lambda_*)}=\boldsymbol{0} \tag{4b}$$

$$\|\boldsymbol{w}\|\neq 0 \tag{4c}$$

where $\boldsymbol{w}$ is the left eigenvector that must be related to the null eigenvalue at the bifurcation point $\lambda=\lambda_*$; and $\boldsymbol{z}_*$ is the state vector at the bifurcation point.

In this paper, the nonzero condition of (4c) is replaced with $\|\boldsymbol{w}\|^2-1=0$ to normalize the left eigenvector. The partial derivatives of the left eigenvector multiplied by the Jacobian matrix in (4b) are calculated from the expanded Jacobian formulation proposed in [26], which uses a variant of the CPF. This formulation uses sigmoid smooth functions to represent the reactive power limits of generators and control devices. The result is a direct method capable of finding both SNB and LIB using the same formulation.

In this paper, only control equations involving Q-limits are considered, as these are the main causes of LIB. Therefore, the expanded Jacobian matrix is given by:

$$\frac{\partial\boldsymbol{f}}{\partial\boldsymbol{z}}=\begin{bmatrix}\dfrac{\partial\boldsymbol{P}}{\partial\boldsymbol{\theta}} & \dfrac{\partial\boldsymbol{P}}{\partial\boldsymbol{V}} & \boldsymbol{0}\\ \dfrac{\partial\boldsymbol{Q}}{\partial\boldsymbol{\theta}} & \dfrac{\partial\boldsymbol{Q}}{\partial\boldsymbol{V}} & \dfrac{\partial\boldsymbol{Q}}{\partial\boldsymbol{Q}_G}\\ \boldsymbol{0} & \dfrac{\partial\boldsymbol{G}}{\partial\boldsymbol{V}} & \dfrac{\partial\boldsymbol{G}}{\partial\boldsymbol{Q}_G}\end{bmatrix} \tag{5}$$

where $\boldsymbol{z}=[\boldsymbol{\theta},\boldsymbol{V},\boldsymbol{Q}_G]^{\mathrm{T}}$; $\boldsymbol{P}$, $\boldsymbol{Q}$, and $\boldsymbol{G}$ are the vectors of active power, reactive power, and mismatches of the controlled variables, respectively; $\boldsymbol{\theta}$ and $\boldsymbol{V}$ are the vectors of bus voltage angles and magnitudes, respectively; and $\boldsymbol{Q}_G$ is the control variable vector for the generated reactive power.

The Q-limit control residue of a synchronous generator connected to bus k can be calculated as:

$$\begin{aligned}\Delta G_k=&(1-ch1\cdot ch3)(1-ch2\cdot ch4)(V_k^{\mathrm{ref}}-V_k^{\mathrm{cal}})+\\&(ch1\cdot ch3)(1-ch2\cdot ch4)(Q_{Gk}^{\max}-Q_{Gk}^{\mathrm{cal}})+\\&(1-ch1\cdot ch3)(ch2\cdot ch4)(Q_{Gk}^{\min}-Q_{Gk}^{\mathrm{cal}})\end{aligned} \tag{6}$$

$$ch1=(1+\mathrm{e}^{a(Q_{Gk}^{\mathrm{cal}}-Q_{Gk}^{\max}+tol)})^{-1} \tag{7a}$$

$$ch2=(1+\mathrm{e}^{a(Q_{Gk}^{\mathrm{cal}}-Q_{Gk}^{\min}-tol)})^{-1} \tag{7b}$$

$$ch3=(1+\mathrm{e}^{a(V_k^{\mathrm{cal}}-V_k^{\mathrm{ref}}-tol)})^{-1} \tag{7c}$$

$$ch4=(1+\mathrm{e}^{a(V_k^{\mathrm{cal}}-V_k^{\mathrm{ref}}+tol)})^{-1} \tag{7d}$$

where $ch1$, $ch2$, $ch3$, and $ch4$ are the sigmoid functions; Q_{Gk}^{cal}, $Q_{Gk}^{\max}$, and $Q_{Gk}^{\min}$ are the calculated, maximum, and minimum values of reactive power of the synchronous generator connected to bus k, respectively; V_k^{ref} and V_k^{cal} are the reference and calculated voltages of bus k, respectively; a is the slope of the sigmoid function; and tol is a tolerance value. To ensure that the outputs of the sigmoid functions are approximately either 0 or 1, a is set to be a large value ($>10^5$) and tol is set to be a small one ($<10^{-4}$).

The objective of the sigmoid functions is to represent the discontinuities related to Q-limits by smooth functions, thus enabling the detection of LIB as SNB in (4) [26]. Since the proposed direct method uses the expanded Jacobian matrix

instead of iteratively converting one *PV*-type bus into a *PQ*-type bus according to the *PV*-*PQ* bus type switching logic when the reactive power limit is reached, such as in [24], it is simpler to implement and results in significant computational time savings.

The nonlinear algebraic equation set (4), hereinafter described by $\boldsymbol{F}(\boldsymbol{Z})=\boldsymbol{0}$, with $\boldsymbol{Z}=[\boldsymbol{z},\lambda,\boldsymbol{w}]$, can be solved by any numerical method. If the classical Newton-Raphson method is used, (4b) must be solved for $\boldsymbol{Z}$, where

$$\frac{\partial \boldsymbol{F}}{\partial \boldsymbol{Z}}=\begin{bmatrix} \dfrac{\partial \boldsymbol{f}}{\partial \boldsymbol{z}} & \dfrac{\partial \boldsymbol{f}}{\partial \lambda} & \boldsymbol{0} \\ \dfrac{\partial\left(\boldsymbol{w}^{\mathrm{T}}\dfrac{\partial \boldsymbol{f}}{\partial \boldsymbol{z}}\right)}{\partial \boldsymbol{z}} & \boldsymbol{0} & \dfrac{\partial\left(\boldsymbol{w}^{\mathrm{T}}\dfrac{\partial \boldsymbol{f}}{\partial \boldsymbol{z}}\right)}{\partial \boldsymbol{w}} \\ \boldsymbol{0} & \boldsymbol{0} & \dfrac{\partial(\|\boldsymbol{w}\|^2-1)}{\partial \boldsymbol{w}} \end{bmatrix} \tag{8}$$

In (8), the terms $\partial \boldsymbol{f}/\partial\lambda$ and $\partial(\|\boldsymbol{w}\|^2-1)/\partial \boldsymbol{w}$ can be replaced with $\boldsymbol{b}_{PL}-\boldsymbol{\alpha}\sum_{i=1}^{N_L} b_{PLi}$ and $2\boldsymbol{w}^{\mathrm{T}}$, respectively, and the term $\partial\left(\boldsymbol{w}^{\mathrm{T}}\partial \boldsymbol{f}/\partial \boldsymbol{z}\right)/\partial \boldsymbol{w}$ is equivalent to $(\partial \boldsymbol{f}/\partial \boldsymbol{z})^{\mathrm{T}}$. Finally, as an extension of [26], the second partial derivative resulting from the application of the Newton-Raphson method to (4b) is calculated as:

$$\frac{\partial\left(\boldsymbol{w}^{\mathrm{T}}\dfrac{\partial \boldsymbol{f}}{\partial \boldsymbol{z}}\right)}{\partial \boldsymbol{z}}=\begin{bmatrix} \dfrac{\partial \boldsymbol{A}}{\partial \boldsymbol{\theta}} & \dfrac{\partial \boldsymbol{A}}{\partial \boldsymbol{V}} & \boldsymbol{0} \\ \dfrac{\partial \boldsymbol{B}}{\partial \boldsymbol{\theta}} & \dfrac{\partial \boldsymbol{B}}{\partial \boldsymbol{V}} & \dfrac{\partial \boldsymbol{B}}{\partial \boldsymbol{Q}_G} \\ \boldsymbol{0} & \dfrac{\partial \boldsymbol{C}}{\partial \boldsymbol{V}} & \dfrac{\partial \boldsymbol{C}}{\partial \boldsymbol{Q}_G} \end{bmatrix} \tag{9}$$

$$\boldsymbol{A}=\frac{\partial \boldsymbol{P}^{\mathrm{T}}}{\partial \boldsymbol{\theta}}\boldsymbol{w}_P+\frac{\partial \boldsymbol{Q}^{\mathrm{T}}}{\partial \boldsymbol{\theta}}\boldsymbol{w}_Q \tag{10a}$$

$$\boldsymbol{B}=\frac{\partial \boldsymbol{P}^{\mathrm{T}}}{\partial \boldsymbol{V}}\boldsymbol{w}_P+\frac{\partial \boldsymbol{Q}^{\mathrm{T}}}{\partial \boldsymbol{V}}\boldsymbol{w}_Q+\frac{\partial \boldsymbol{G}^{\mathrm{T}}}{\partial \boldsymbol{V}}\boldsymbol{w}_{\boldsymbol{Q}_G} \tag{10b}$$

$$\boldsymbol{C}=\frac{\partial \boldsymbol{Q}^{\mathrm{T}}}{\partial \boldsymbol{Q}_G}\boldsymbol{w}_Q+\frac{\partial \boldsymbol{G}^{\mathrm{T}}}{\partial \boldsymbol{Q}_G}\boldsymbol{w}_{\boldsymbol{Q}_G} \tag{10c}$$

where $\boldsymbol{w}_P$, $\boldsymbol{w}_Q$, and $\boldsymbol{w}_{\boldsymbol{Q}_G}$ are the partitions of the left eigenvector $\boldsymbol{w}$ corresponding to active power, reactive power, and generated reactive power (as a controlled variable), respectively.

III. Models of Uncertainties in Load and Intermittent Generation and Proposed Approach Based on CE Method

This section defines the uncertainty models for load growth direction and intermittent generation output power, including their stochastic dependence, which is an important feature that must be considered in voltage security assessment. For simplicity, only wind power generation is considered in this paper, although additional uncertain models representing other types of intermittent generators can be easily incorporated into the adapted CE method presented in Section III-D. Furthermore, the use of an approach based on the CE method is justified. Accordingly, the CE method is also presented, incorporating the adaptions introduced in this study.

The uncertainty models are based on normal distributions and Gaussian copulas, which are suitable for the voltage security study in this paper. As demonstrated in [29], the Brazilian National System Operator considered historical wind power generation data from the northeast region of Brazil and concluded that, when viewed as a group of multiple wind farms, wind power generation conformed to a normal distribution. In [30], similar conclusions were reached, based on the premise of a large number and geographical dispersion of wind turbines. This same reasoning can be extended to load models. Furthermore, employing the Gaussian copula to characterize correlations between input variables is supported by recent studies on voltage and small-disturbance stability based on actual system datasets, such as [31].

A. Uncertain Model of Load Growth Direction

Among the multiple load growth models in the literature, a normal probability distribution function (PDF) $p(b_{PLi})$ given by (11) is used in works such as [12] and [13].

$$p(b_{PLi})=\frac{1}{\sqrt{2\pi\sigma_{b_{PLi}}^2}}\exp\left(-\frac{(b_{PLi}-\mu_{b_{PLi}})^2}{2\sigma_{b_{PLi}}^2}\right) \tag{11}$$

where $\mu_{b_{PLi}}$ and $\sigma_{b_{PLi}}$ are the mean and the standard deviation of directions of load increase at bus i, respectively. To maintain a constant power factor, reactive power increases in proportion to active power.

B. Uncertain Model of Wind Power Generation

This paper follows a line similar to the one adopted in [29] for modeling wind power generation, which is represented by power injections from wind farm groups, modeled as stochastic variables with a normal PDF $p(P_{Wi})$ given by (12).

$$p(P_{Wi})=\frac{1}{\sqrt{2\pi\sigma_{P_{Wi}}^2}}\exp\left(-\frac{(P_{Wi}-\mu_{P_{Wi}})^2}{2\sigma_{P_{Wi}}^2}\right) \tag{12}$$

where $\mu_{P_{Wi}}$ and $\sigma_{P_{Wi}}$ are the mean and the standard deviation of wind power generation at bus i, respectively; and P_{Wi} is the component of wind power generation vector $\boldsymbol{P}_W$.

C. Stochastic Dependence Among Uncertainties

A detailed analysis of the dependence (correlation) of stochastic variables used in voltage security assessment can be found in [31]. This study reveals that load-to-load uncertainties are highly dependent, whereas the correlations between system load and wind speed uncertainties are very weak. This is reasonable given that the consumption pattern of system loads (customers) is typically unrelated to the natural variation of wind speed. In terms of wind speed to wind speed interdependence, this study highlights that the correlation decreases as the distance between wind farms increases. This allows us to neglect the load-to-wind dependence in our representation of the correlation among uncertainties by a Gaussian copula given by (13).

$$f(\boldsymbol{X},\boldsymbol{\mu},\boldsymbol{\Sigma})=\frac{1}{|\boldsymbol{\Sigma}|(2\pi)^d}\exp\left(-\frac{1}{2}(\boldsymbol{X}-\boldsymbol{\mu})\boldsymbol{\Sigma}^{-1}(\boldsymbol{X}-\boldsymbol{\mu})^{\mathrm{T}}\right) \quad (13)$$

where $\boldsymbol{X}=[\boldsymbol{b}_{PL},\boldsymbol{P}_W]$; $\boldsymbol{\mu}=[\boldsymbol{\mu}_{\boldsymbol{b}_{PL}},\boldsymbol{\mu}_{\boldsymbol{P}_W}]$, and $\boldsymbol{\mu}_{\boldsymbol{b}_{PL}}=(\mu_{b_{PLi}})$, $\boldsymbol{\mu}_{\boldsymbol{P}_W}=(\mu_{P_{Wi}})$; $\boldsymbol{\Sigma}$ is a symmetric, positive definite matrix with a dimension of $d\times d$; and $|\boldsymbol{\Sigma}|$ is the determinant of $\boldsymbol{\Sigma}$.

D. Overview of Proposed Approach Based on CE Method

In voltage security assessment, the system is considered insecure if the VSM is smaller than a certain threshold, which will be represented in this paper by $S(\boldsymbol{X})\le\gamma$. $S(\boldsymbol{X})$ is the load margin for a given $\boldsymbol{X}$. For instance, the Brazilian National System Operator in Brazil defines this threshold as $\gamma=7\%$ for the base case and $\gamma=4\%$ for contingency analyses [32]. Although violations of these security margins can make the system vulnerable to serious outage events with high impact, the probability of these violations is typically low [13], [33]. This justifies our decision to assess the risk of voltage insecurity (and instability, consequently) using the CE method.

CE-based approaches, which involve variance minimization, are known for their effectiveness in estimating probabilities of rare events. Some CE-based power system applications include constrained optimal power flow solutions [15], [16], spinning reserve assessment under transmission constraints [34], and identification of critical scenarios from the voltage stability viewpoint [17], [18].

A brief overview of the proposed approach based on the CE method is given below. For details on the general fundamentals of the CE method, see [35]. Let a probability ℓ for some measurable functions of an event $S(\boldsymbol{X})\le\gamma$, $\gamma\in\mathbb{R}$ (i.e., the expectation defined by a collection of indicator functions, $\mathbb{E}[I_{\{S(\boldsymbol{X})\le\gamma\}}]$) be defined as:

$$\ell=\int I_{\{S(\boldsymbol{X})\le\gamma\}}f(\boldsymbol{X};\boldsymbol{u})\mathrm{d}\boldsymbol{X}\quad \boldsymbol{X}\sim f(\cdot,\boldsymbol{u}) \quad (14)$$

where $f(\boldsymbol{X};\boldsymbol{u})$ is the PDF of $\boldsymbol{X}$ determined by a parameter vector $\boldsymbol{u}$; $f(\cdot,\boldsymbol{u})$ is the general form of this PDF over its entire domain; and $I_{\{S(\boldsymbol{X})\le\gamma\}}$ is the indicator function with a 0 (false) or 1 (true) result.

The MCS method produces an estimation $\hat{\ell}$ of ℓ given by (15), which defines an unbiased estimator from N random samples $X_1,X_2,\ldots,X_N$ of a distribution of $\boldsymbol{X}$.

$$\hat{\ell}=\frac{1}{N}\sum_{k=1}^{N}I_{\{S(X_k)\le\gamma\}} \quad (15)$$

Consider a new probability distribution $g(\boldsymbol{X};\boldsymbol{v})$ such that ℓ can be expressed as (16) and $\hat{\ell}$ can be estimated by (17).

$$\ell=\int I_{\{S(\boldsymbol{X})\le\gamma\}}W(\boldsymbol{X},\boldsymbol{u},\boldsymbol{v})g(\boldsymbol{X};\boldsymbol{v})\mathrm{d}\boldsymbol{X}\quad \boldsymbol{X}\sim g(\cdot,\boldsymbol{v}) \quad (16)$$

$$\hat{\ell}=\frac{1}{N}\sum_{k=1}^{N}I_{\{S(X_k)\le\gamma\}}W(X_k,\boldsymbol{u},\boldsymbol{v}) \quad (17)$$

where $g(\boldsymbol{X};\boldsymbol{v})$ is the PDF of $\boldsymbol{X}$ determined by a parameter vector $\boldsymbol{v}$; $g(\cdot,\boldsymbol{v})$ is the general form of this PDF over its entire domain; and $W(\boldsymbol{X},\boldsymbol{u},\boldsymbol{v})=f(\boldsymbol{X};\boldsymbol{u})/g(\boldsymbol{X};\boldsymbol{v})$ is the likelihood ratio of PDFs.

The random samples are now drawn from the PDF $g(\boldsymbol{X})$ according to (17). Hence, the estimation of the PDF $g(\boldsymbol{X})$ forms the basis of the importance sampling techniques. As discussed in Section III-C, in this paper, the used sampling distributions are multivariate normal PDF. In this case, a fast way to determine $g(\boldsymbol{X})$ is to select a distribution equivalent to $f(\boldsymbol{X})$. To this end, Algorithm 1 describes a procedure based on CE method to find $g(\boldsymbol{X})\sim f(\boldsymbol{X};\boldsymbol{v})$ from the original distribution $f(\boldsymbol{X};\boldsymbol{u})$. This algorithm is an adaptation of the original one in [35], with PDF normalization and changes to the convergence criteria. As a result, the computational cost is reduced while also minimizing the potential problems associated with finding a correlation matrix that is not positive definite. It is important to remark that the Cholesky decomposition is required only in the first iteration, so the computational burden of the algorithm is not significantly affected by this decomposition.

Algorithm 1: procedure based on CE method to find $g(\boldsymbol{X})\sim f(\boldsymbol{X};\boldsymbol{v})$ from the original distribution $f(\boldsymbol{X};\boldsymbol{u})$

Step 1: from $\boldsymbol{X}$ and its respective PDF $f(\boldsymbol{X};\boldsymbol{u})$, generate a set of random samples X_j, $j=1,2,\ldots,m$ (m is the number of samples drawn from the distribution of $\boldsymbol{X}$). Convert the random samples X_j into standard normal values Z_j and adjust each Z_j to match the original distribution correlation structure using the Cholesky decomposition. Set the iteration number $it=1$ and $\hat{\boldsymbol{v}}_1=\boldsymbol{u}$. $\hat{\boldsymbol{v}}_1$ is the estimator of $\boldsymbol{v}_1$.

Step 2: calculate the performances $S(X_j)$ and select the elements X_e, $e=1,2,\ldots,m_e$ of the elite set, where m_e is determined by the p^{th} percentile of m sorted in ascending order of their respective $S(X_e)$.

Step 3: if $S(X_{m_e})\le\gamma$, set $\hat{\boldsymbol{v}}=\hat{\boldsymbol{v}}_{it}$ and stop. $\hat{\boldsymbol{v}}$ and $\hat{\boldsymbol{v}}_{it}$ are the estimators of the final $\boldsymbol{v}$ and the $\boldsymbol{v}$ at iteration it, respectively. Otherwise, set $it=it+1$ and convert the samples X_e into standard normal values Z_e.

Step 4: update the parameters $\boldsymbol{\mu}_{it}$ and $\boldsymbol{\Sigma}_{it}$ of $\hat{\boldsymbol{v}}_{it}$ using Z_e. Then, from PDF $f(\boldsymbol{Z},\hat{\boldsymbol{v}}_{it})$, generate new random samples Z_j, $j=1,2,\ldots,m$. Convert the standard random samples Z_j into normal values X_j using PDF $f(\boldsymbol{X};\boldsymbol{u})$. Reiterate from *Step 2*.

IV. Proposed Definition of Contingency Criticality

In Section III, the modeling necessary to analyze the risk of voltage insecurity (and instability, consequently) is introduced, with the load and intermittent generation uncertainties represented as PDF. As discussed in this same section, power systems typically operate with a large VSM, so violations of this margin are rare events, justifying the use of the CE method. Naturally, as the risk of violation increases, the benefits of the CE method over the traditional MCS method diminish, though it should still prevail to some extent. This section summarizes the proposed approach for defining contingency criticality.

Voltage security and stability studies must be conducted preserving the system structure (without contingencies) and with selected contingencies, considering multiple scenarios of correlated uncertainties. Therefore, to deal with the large number of simulations required, the direct method proposed in Section II is implemented to compute the VSM with an expanded Jacobian matrix, considering the Q-limits of the synchronous generators, as described in Section II-B. The main advantage of this implementation lies in its ability to convert LIB points to SNB points, making them equally identifiable.

The flowchart in Fig. 1 summarizes the stages needed to implement the proposed approach. The input data consist of: ① network data with line and bus parameters, including the Q-limits of synchronous generators; ② the number of samples used in each stage of the CE method and the percentage of the elite samples; ③ parameters of the direct method, such as the maximum mismatch (error) for Newton-Raphson convergence; ④ the mean vector and correlation matrix of the multivariate normal distribution obtained from the PDFs of load growth direction and wind power generation; and ⑤ the lines that will be switched off in contingency analysis. In the flowchart, the variable c represents the contingency number in the list, with $c=0$ indicating no contingency.

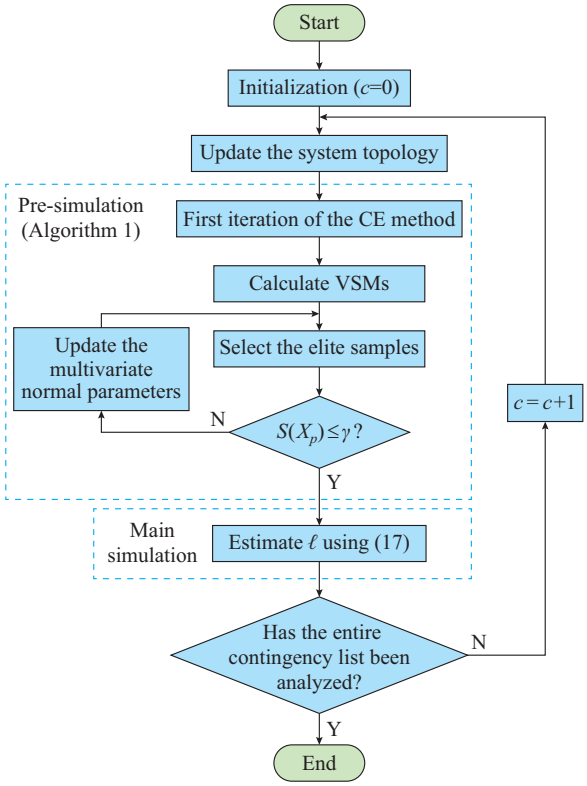

Fig. 1. Flowchart to implement proposed approach.

In the remainder of this paper, Algorithm 1 will be referred to as the pre-simulation stage. The initialization of the proposed approach generates scenarios (samples) with consumed power from loads and injected power from wind farms using a multivariate normal distribution. For each uncertain scenario and system topology, the direct method is executed to compute the VSM. As a result, the elite samples are selected from scenarios with the smallest margins. If none of the elite samples violates the VSM, the parameters of the multivariate distribution are updated. New samples are then drawn from the updated parameters after a normalization process. Conversely, if a violation occurs, the violation probability of the VSM is calculated using the parameters of the current (converged) iteration of the pre-simulation stage. If this stage requires more than one iteration, the likelihood ratio vector must be computed to correct the estimated violation probability of the VSM. This procedure is repeated for all topologies and scenarios in the contingency list.

After the convergence of the pre-simulation stage, the main simulation stage of the proposed approach produces a list with the violation probabilities of the VSM for all uncertain operating conditions contained in the contingency list. Based on these probabilities, a new definition of contingency criticality is proposed as follows.

Definition When correlated uncertainties under the operating condition are considered, the criticality of the selected contingencies must be ranked in descending order of their respective violation probabilities of the VSM.

As will be shown later in Section V, the main innovation and advantage of this new definition is its compliance with grid codes. Although contingencies happening under operating conditions given by the base case may not result in a violation of the respective VSM, when uncertainties under these conditions are considered, the probability of such violation can be quite significant. Therefore, under this framework with correlated uncertainties, a contingency is considered critical if it creates a violation probability of the VSM. This new definition aligns with grid codes, as it captures the possibility of margin violations due to uncertainties, even if no violations are observed in the base case. An illustrative example of this concept is given in Section V-B.

V. Simulation Results

Initially, the proposed approach and its advantages are comprehensively explained on a 5-bus test system. As a proof of concept, the bifurcation surface is shown both with and without Q-limit consideration. Furthermore, the results of the violation probability of the VSM obtained from the proposed approach are compared with those obtained using the MCS method to verify the accuracy and computational efficiency of the former. Although these are known facts in a general sense, this verification is still necessary due to the unique characteristics of the voltage stability problem, which involves a nonlinear equation set. Then, the proposed definition is applied to the IEEE 118-bus test system, which is modified by the addition of seven wind farms. The test results include contingency scenarios, given by topology changes, in addition to the current topology scenario. The violation percentages of $\gamma=7\%$ and $\gamma=4\%$ are used for cases in which the system topology is complete and under contingency, respectively [32]. This application to the IEEE 118-bus test system enables an assessment of the advantages of the proposed definition.

A. Application of Proposed Approach to a 5-bus Test System

As shown in Fig. 2, the 5-bus test system has generators at buses 1 and 3 and loads at buses 2, 4, and 5. The line parameters and the generator parameters are extracted from [27]. Since the primary goal is to validate the proposed approach, a small system without wind farm is considered. To put the system under a stressed operating condition, in the base case, the active and reactive power values consumed by the loads given in [27] are multiplied by 1.7 times their nominal values. Since this test system only has one *PV*-type bus, we chose a redispatch model in which this bus supplies 23%

of the load growth. Furthermore, the reactive power of the generator at bus 3 is limited to 2.5 p.u.. As a result, in the scenario with no uncertainties, the load margin is 8.69%.

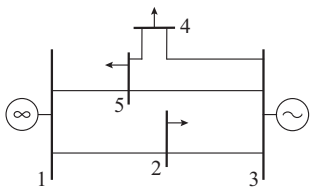

Fig. 2. One-line diagram of 5-bus test system.

The parameter space of load active power is mapped in $\mathbb{R}^3$ with b_{PLi}, $i=2,4,5$, ranging from 0 to 1 in intervals of 0.1 p.u. (excluding the direction with no growth), which results in 1330 different load growth directions. All load growths start from the left front corner of Fig. 3, where P_{L_2}, P_{L_4}, and P_{L_5} are the components of $\boldsymbol{P}_L$ in (2) applied to the 5-bus test system of Fig. 2. The black area in Fig. 3 is an interpolation of the bifurcation surface calculated without Q-limits, while the gray area is an interpolation of the bifurcation surface calculated with Q-limits. Figure 3 clearly shows that Q-limits significantly reduce the VSM in all load growth directions.

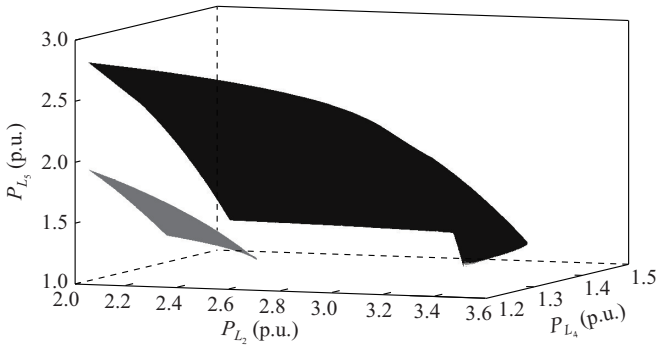

Fig. 3. Bifurcation surfaces of 5-bus test system with and without Q-limits.

When uncertainties in the load growth direction are considered, the cases that contain violations of VSMs become even rarer events. Table I displays the calculated probability of violating the VSM of 7%, i.e., Pr($VSM<7\%$). Naturally, results obtained using a large sample with the MCS method provide a more accurate estimate. In this table, the violation probabilty results are determined using various $\boldsymbol{b}_{PL}$ that are modeled using a normal distribution with a standard deviation equal to 30% of the nominal load values. For testing and comparison purposes, the correlation matrix among load buses is defined using Pearson correlation coefficients ρ [36], which are equal to 0 (no correlation), 0.4, and 0.8. The time shown in this table is obtained by simulation on the MATLAB 2022.b, using a PC with an Intel Core i7-14700 2.1 GHz processor and 32 GB RAM.

In comparison, the results using the proposed approach is shown in Table II. These results are obtained with $m=750$ and $p=0.1$ [15] for the pre-simulation stage and 3000 samples for the main simulation stage.

TABLE I
RESULTS OF MCS METHOD WITH DIFFERENT NUMBER OF SAMPLES

ρ	3000 samples		10^6 samples	
	Pr($VSM<7\%$)	Time (s)	Pr($VSM<7\%$)	Time (s)
0	5.53	4.40	5.42	3180.87
0.4	2.80	4.30	2.68	2099.43
0.8	0.60	4.23	0.48	1813.29

Assuming that the solutions using the MCS method in Table I achieve satisfactory accuracy for the case with 10^6 samples, it is possible to see that the proposed approach presents more accurate solutions than the MCS method with 3000 samples, requiring slightly higher computational time. Furthermore, when compared to the results of the MCS method using 10^6 samples, the advantages of the proposed approach in terms of the tradeoff between accuracy and computational time become evident.

TABLE II
RESULTS OF PROPOSED APPROACH

ρ	Pr($VSM<7\%$)	Time (s)
0	5.38	6.91
0.4	2.55	6.69
0.8	0.45	6.66

The results of Tables I and II for $\rho=0.8$ are divided into four intervals to provide more detailed results, as shown in Fig. 4. Each interval is defined by the range of the VSM for each respective sample, as described by the legend. Note that the result of the proposed approach is the closest one to that of the MCS method with 10^6 samples in all intervals. Therefore, Fig. 4 shows that the proposed approach generates accurate results for any desired range of violation of the VSM.

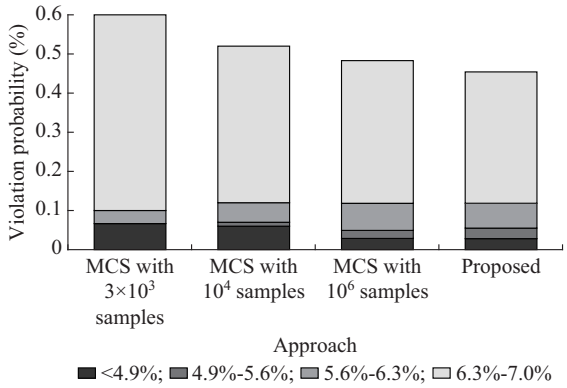

Fig. 4. Results from MCS method and proposed approach for $\rho=0.8$.

B. Application of Proposed Definition to IEEE 118-bus Test System

The proposed approach is applied to contingency analysis using the IEEE 118-bus test system in Fig. 5, in such a way that the proposed definition can effectively be tested. The active power and reactive power of 99 loads are increased by

a factor of 2.15 over the original system values to make the power system more stressed, and 7 wind farms are added to buses 8, 32, 42, 55, 76, 92, and 105. Each wind farm is set to inject 200 MW of active power. The total amount of power produced by wind farms supplies 15% of the total demand of the system for the base case, which leads to a VSM of 11.54% for the system.

The violation probability of the VSM for the system under contingency is determined with the consideration of uncertainties in 99 active power increment values consumed by loads and 7 active power values injected by wind farms. $\boldsymbol{b}_{PL}$ is modeled as a normal PDF with a mean value described by the load active power of the base case and a standard deviation defined as 10% of this mean value. The power injected by each wind farm is modeled as a normal PDF with a mean value equal to 200 MW and a standard deviation equal to 25% of this mean value. To determine the correlation matrix, this system is first divided into six electrical areas, as shown in Fig. 5. To model load uncertainties, considering that the loads are tightly coupled electrically and geographically, $\rho = 0.8$ is used for loads in the same area, $\rho = 0.6$ is used for loads in adjacent areas, and $\rho = 0.4$ otherwise.

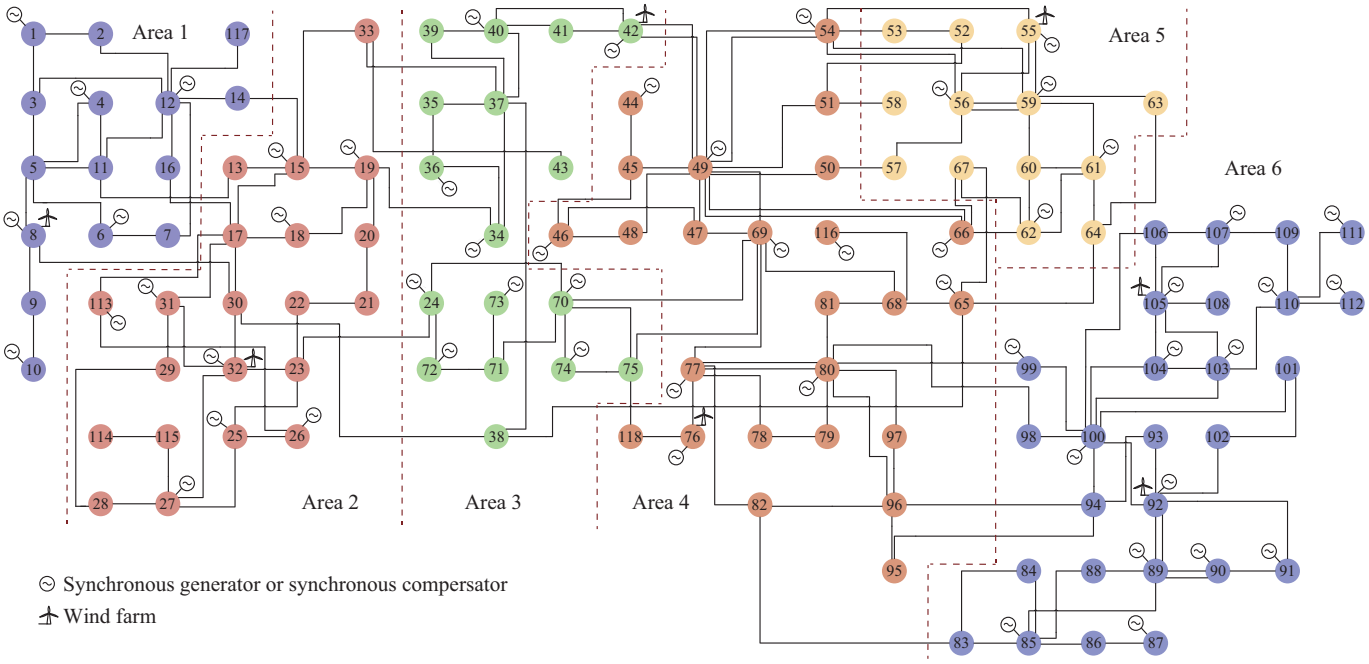

Fig. 5. One-line diagram of IEEE 118-bus test system.

The correlation among wind farms, on the other hand, is dependent on their physical proximity. To model this uncertainty, $\rho = 0.3$ is used for the groups of wind farms connected to buses (8; 32), (42; 55; 76), and (92; 105). The autocorrelation of each wind farm is modeled by $\rho = 1$, and no correlation ($\rho = 0$) is considered both between wind farms and loads and between groups of wind farms.

The proposed approach uses 1000 samples and $p = 0.1$ for the pre-simulation stage and 10000 samples for the main simulation stage. In some cases, the pre-simulation stage converges in the first iteration, which indicates that the corresponding events are not rare. In these cases, the parameter $\hat{\boldsymbol{v}}$ is equal to $\boldsymbol{u}$ and, therefore, the PDF $f(\boldsymbol{X};\boldsymbol{u})$ is suitable for the main simulation stage. Non-rare contingencies must also be ranked, so the number of samples must be carefully chosen to avoid biased estimation by the proposed approach. Based on the approach presented in [21], the chosen sample sizes are adequate to produce an unbiased ranking with a mean sampling error of less than 0.01 for a 99% confidence interval. However, different choices may optimize the estimation depending on the number of parameters and the size of the associated stochastic problem, so this issue must be further investigated in applications of the proposed approach to other system models, which is currently underway.

Table III shows the results of the proposed definition, i.e., the list of critical contingencies in descending order according to the proposed definition to evaluate criticality. For simplicity, only the disconnection of lines is considered in the contingency analysis. In Table III, the third column contains the violation probability of the VSM that is used to rank the criticality of the contingency considering uncertainties under the operating conditions.

The results in Table III clearly illustrate the importance of considering the proposed definition to adequately rank the contingency list in terms of criticality. If the criterion used to define criticality is the VSM of the base case (which is typically done by system operators), only the contingencies in lines 74-75 and 45-46 would be labeled as critical. Furthermore, the contingencies in lines 22-23 and 44-45 would be prioritized with respect to the ones in lines 75-118, 69-70, and 69-75. These issues could lead to insufficient preventive control actions being identified to eliminate the critical contingencies in voltage security assessment studies.

Voltage security analysis, like most other problems in the security assessment of power systems, is highly dependent on the operating conditions. Therefore, as expected, the pro-

posed ranking of contingency criticality does not exhibit a universal pattern. To illustrate this, the first five contingencies (identified as the most critical ones in Table III) for the same system are now analyzed under a less heavily loaded condition. Instead of the original factor of 2.15, which is used to create Table III, the loads are increased by a factor of 2.10 with respect to their original values in [37], changing the mean values and variances of the uncertain load models. The wind farms maintain 200 MW of active power injection with no changes in the uncertainty settings. With these modifications, the wind power generation accounts for approximately 16% of the power demand, and the base case (without uncertainties) exhibits a VSM of 14.17%.

TABLE III
RESULTS OF PROPOSED DEFINITION APPLIED TO 118-BUS TEST SYSTEM

Line under contingency	VSM of base case (%)	Pr($VSM < 4\%$) with uncertainty (%)
Line 74-75*	2.07	93.84
Line 45-46*	4.05	53.95
Line 75-118*	6.12	21.73
Line 69-70*	6.49	13.84
Line 69-75*	6.72	11.25
Line 44-45	5.66	4.56
Line 85-89	6.23	3.43
Line 22-23	5.32	2.45
Line 85-88	7.17	1.07

Note: * denotes that the pre-simulation stage converges in the first iteration.

Table IV presents the results of the proposed definition applied to this different base case. It is interesting to observe that no contingency would be classified as critical under the widely accepted deterministic definition, which is the VSM of the base case (shown in second column of Table IV). However, the application of the proposed definition reveals that the contingencies involving lines 74-75 and 75-118 have a higher than 10% probability of violating the VSM. Furthermore, for the contingency involving line 45-46, the violation probability of the VSM sharply decreases, which affects the ranking with respect to Table III. These results clearly show the dependency of both the deterministic and the proposed definition of contingency criticality on the system operating conditions.

TABLE IV
RESULTS OF PROPOSED DEFINITION APPLIED TO 118-BUS TEST SYSTEM UNDER ANOTHER OPERATING CONDITION

Line under contingency	VSM of base case (%)	Pr($VSM < 4\%$) (%)	
		Proposed approach	MCS method with 10^5 samples
Line 74-75*	4.55	41.24	41.40
Line 75-118*	8.69	11.87	11.64
Line 45-46	6.57	2.54	2.93
Line 69-70	9.10	1.31	1.79
Line 69-75	9.32	0.88	0.90

Note: * denotes that the pre-simulation converges in the first iteration.

Table IV is also used to present a comparison of the results produced by the proposed approach with the ones generated by a benchmark, which is chosen as the MCS method with 10^5 samples to the same problem. It is possible to see that the proposed approach accurately estimates the violation probabilities of the VSM for all the analyzed contingencies with respect to the benchmark for both rare and non-rare events. Furthermore, the average time taken to produce the results of Table IV with the proposed approach is 10040 s. This is a reduction of more than 90% of the average time of 132233 s taken to produce the respective results with the MCS method, which demonstrates the computational efficiency of the proposed approach. It is important to remark that the average time taken for the proposed approach to produce the results is adequate for day-ahead operation planning; however, if shorter time windows or larger systems are required, the proposed approach offers several possibilities to apply parallel and/or distributed computation, so the scalability of the approach is suitable to handle more computationally demanding problems.

In summary, the proposed definition reveals that contingencies with a satisfactory VSM in the base case can have a high violation probability of the VSM due to the uncertainties under the operating conditions. Therefore, it is possible to tailor a threshold for the contingency analysis of interest—depending on the system and its uncertain features, as well as the level of conservatism required by the operator (given that stability and security are at stake)—to consider a violation probability above which all contingencies must be taken into account for the determination of preventive control actions.

VI. CONCLUSION

The results of this paper demonstrate the need for the adaptation of voltage stability and security assessment methods to the current trends in the operation of power systems, mainly with respect to uncertainties. In particular, the proposed definition of contingency criticality shows that contingencies with satisfactory VSMs in the base case can become critical due to uncertainties under the operating conditions. Thus, with a careful selection of a threshold for the violation probability of the VSM defined in the respective grid code, it is possible to select and rank the most critical contingencies from the list of those assessed.

However, since uncertainties are considered in the problem formulation, the computational burden to solve it increases. Therefore, to handle this issue, strategies to speed up the solution must be employed. This paper is particularly successful in achieving a satisfactory tradeoff between computational effort and accuracy of the results by proposing an approach based on the CE method to calculate the violation probabilities of the VSM. Furthermore, the use of a modified version of the direct method to calculate the VSM also results in a reduction of the computational burden.

The proposed definition can be applied to the selection of preventive control actions to eliminate the criticality of all contingencies. Furthermore, the definition can be extended to simultaneously assess voltage and small-signal stability

and security if Hopf bifurcations are considered in the formulation presented in Section II.

Currently, the development of general guidelines for defining the number of samples in both the pre-simulation and main simulation stages of the proposed approach is under investigation. Future directions of this research include an extension of this paper to consider different uncertainty models within a large class of parametric distributions, which is currently underway, as well as the incorporation of more limits that may impact voltage stability, other than *Q*-limits of the synchronous generators.

REFERENCES

[1] J. V. Milanovic, R. Preece, and K. N. Hasan, *Probabilistic Stability Analysis of Uncertain Power Systems*. Hoboken: Wiley-Interscience, 2024.

[2] L. Fucuchima. (2023, Nov.). Power consumption in Brazil exceeds record 100 GW amid heatwave. [Online]. Available: https://www. marketscreener. com/quote/currency/EURO-BRAZILIAN-REAL-EUR-B-2358324/news/Power-consumption-in-Brazil-exceeds-record-100-GW-amid-heatwave-45352856/? utm_source=copy&utm_medium=social&utm_campaign=share

[3] N. Hatziargyriou, J. Milanovic, C. Rahmann *et al*., "Definition and classification of power system stability – revisited & extended," *IEEE Transactions on Power Systems*, vol. 36, no. 4, pp. 3271-3281, Jul. 2021.

[4] Y. Lin, X. Zhang, J. Wang *et al*., "Voltage stability constrained optimal power flow for unbalanced distribution system based on semidefinite programming," *Journal of Modern Power Systems and Clean Energy*, vol. 10, no. 6, pp. 1614-1624, Nov. 2022.

[5] M. Mansour, L. Alberto, and R. Ramos, "Preventive control design for voltage stability considering multiple critical contingencies," *IEEE Transactions on Power Systems*, vol. 31, no. 2, pp. 1517-1525, Mar. 2016.

[6] V. Ajjarapu and C. Christy, "The continuation power flow: a tool for steady state voltage stability analysis," *IEEE Transactions on Power Systems*, vol. 7, no. 1, pp. 416-423, Feb. 1992.

[7] R. M. Silva, M. F. Castoldi, A. Goedtel *et al*., "Binary differential evolution applied to the optimization of the voltage stability margin through the selection of corrective control sets," *Soft Computing*, vol. 28, no. 15, pp. 8861-8887, Aug. 2023.

[8] B. Shakerighadi, F. Aminifar, and S. Afsharnia, "Power systems wide-area voltage stability assessment considering dissimilar load variations and credible contingencies," *Journal of Modern Power Systems and Clean Energy*, vol. 7, no. 1, pp. 78-87, Jan. 2019.

[9] Y. Chi, A. Tao, X. Xu *et al*., "An adaptive many-objective robust optimization model of dynamic reactive power sources for voltage stability enhancement," *Journal of Modern Power Systems and Clean Energy*, vol. 11, no. 4, pp. 1756-1769, Jul. 2023

[10] D. Guo, L. Wang, T. Jiao *et al*., "Day-ahead voltage-stability-constrained network topology optimization with uncertainties," *Journal of Modern Power Systems and Clean Energy*, vol. 12, no. 3, pp. 730-741, May 2024

[11] Y. Kataoka, "A probabilistic nodal loading model and worst case solutions for electric power system voltage stability assessment," *IEEE Transactions on Power Systems*, vol. 18, no. 4, pp. 1507-1514, Nov. 2003.

[12] X. Xu, Z. Yan, M. Shahidehpour *et al*., "Power system voltage stability evaluation considering renewable energy with correlated variabilities," *IEEE Transactions on Power Systems*, vol. 33, no. 3, pp. 3236-3245, May 2018.

[13] B. Tan, J. Zhao, and L. Xie, "Transferable deep kernel emulator for probabilistic load margin assessment with topology changes, uncertain renewable generations and loads," *IEEE Transactions on Power Systems*, vol. 38, no. 6, pp. 5740-5754, Nov. 2023.

[14] C. Xia, X. Zheng, L. Guan *et al*., "Probability analysis of steady-state voltage stability considering correlated stochastic variables," *International Journal of Electrical Power & Energy Systems*, vol. 131, p. 107105, Oct. 2021.

[15] L. de Magalhaes-Carvalho, A. M. L. da Silva, and V. Miranda, "Security-constrained optimal power flow via cross-entropy method," *IEEE Transactions on Power Systems*, vol. 33, no. 6, pp. 6621-6629, Nov. 2018.

[16] A. M. L. da Silva and A. M. de Castro, "Risk assessment in probabilistic load flow via Monte Carlo simulation and cross-entropy method," *IEEE Transactions on Power Systems*, vol. 34, no. 2, pp. 1193-1202, Mar. 2019.

[17] L. M. Alburguetti, R. M. Silva, A. P. Grilo-Pavani *et al*., "Assessment of critical scenarios for voltage stability considering uncertainty of wind power generation," in *Proceeding of 2022 IEEE PES General Meeting*, Denver, USA, Jul. 2022, pp. 1-5.

[18] M. R. Nascimento, F. A. Ramos, L. C. Almeida *et al*., "Computation of the minimum voltage stability margin considering loading uncertainties and contingency analysis," in *Proceeding of 2023 IEEE PES General Meeting*, Orlando, USA, Jul. 2023, pp. 1-5.

[19] L. S. Neves and L. F. C. Alberto, "On the computation of the locally closest bifurcation point considering loading uncertainties and reactive power limits," *IEEE Transactions on Power Systems*, vol. 35, no. 5, pp. 3885-3894, Sept. 2020.

[20] E. Haesen, C. Bastiaensen, J. Driesen *et al*., "A probabilistic formulation of load margins in power systems with stochastic generation," *IEEE Transactions on Power Systems*, vol. 24, no. 2, pp. 951-958, May 2009.

[21] B. Qi, K. N. Hasan, and J. V. Milanovic, "Identification of critical parameters affecting voltage and angular stability considering load-renewable generation correlations," *IEEE Transactions on Power Systems*, vol. 34, no. 4, pp. 2859-2869, Jul. 2019.

[22] J. Zhang, L. Fan, Y. Zhang *et al*., "A probabilistic assessment method for voltage stability considering large scale correlated stochastic variables," *IEEE Access*, vol. 8, pp. 5407-5415, Dec. 2019.

[23] Y. Yang, S. Lin, Q. Wang *et al*., "Optimization of static voltage stability margin considering uncertainties of wind power generation," *IEEE Transactions on Power Systems*, vol. 37, no. 6, pp. 4525-4540, Nov. 2022.

[24] T. Jiang, K. Wan, and Z. Feng, "Boundary-derivative direct method for computing saddle node bifurcation points in voltage stability analysis," *International Journal of Electrical Power & Energy Systems*, vol. 112, pp. 199-208, Nov. 2019.

[25] K. Wan and T. Jiang, "Augmented system for detecting the steady-state voltage stability margin," *IET Generation*, *Transmission & Distribution*, vol. 14, no. 21, pp. 4788-4795, Nov. 2020.

[26] J. P. P. Barbosa and J. A. P. Filho, "New methodologies for SVC modeling in the power flow problem based on sigmoid functions," *Electrical Engineering*, vol. 106, no. 1, pp. 971-981, Sept. 2023.

[27] I. Dobson and L. Lu, "New methods for computing a closest saddle node bifurcation and worst case load power margin for voltage collapse," *IEEE Transactions on Power Systems*, vol. 8, no. 3, pp. 905-913, Aug. 1993.

[28] E. de Mello-Magalhães, A. B. Neto, and D. A. Alves, "A parameterization technique for the continuation power flow developed from the analysis of power flow curves," *Mathematical Problems in Engineering*, vol. 2012, no. 1, p. 762371, Jan. 2012.

[29] D. M. Falcao and G. N. Taranto. (2023, May). Impact of the connections of large-scale wind and solar generation in the Brazilian interconnected power system. [Online]. Available: https://www.e-papers.com.br/produto/impact_of_the_connections_of_largescale_wind_and_solar_generation_/?v=7efdfc94655a

[30] F. Bouffard and F. D. Galiana, "Stochastic security for operations planning with significant wind power generation," *IEEE Transactions on Power Systems*, vol. 23, no. 2, pp. 306-316, May 2008.

[31] M. Alzubaidi, K. N. Hasan, and L. Meegahapola, "Probabilistic steady-state and short-term voltage stability assessment considering correlated system uncertainties," *Electric Power Systems Research*, vol. 228, p. 110008, Mar. 2024.

[32] ONS – Operador Nacional do Sistema Eletrico, *Procedimentos de Rede – Submdulo 2.3 – Premissas, Criterios e Metodologia Para Estudos Eletricos (in Portuguese)*, PRD-2.3-RO, 2022.

[33] A. M. L. da Silva, I. P. Coutinho, A. C. Z. de Souza *et al*., "Voltage collapse risk assessment," *Electric Power Systems Research*, vol. 54, no. 3, pp. 221-227, Jun. 2000.

[34] A. M. L. da Silva, J. F. C. Castro, and R. A. Gonzalez-Fernandez, "Spinning reserve assessment under transmission constraints based on cross-entropy method," *IEEE Transactions on Power Systems*, vol. 31, no. 2, pp. 1624-1632, Mar. 2016.

[35] R. Y. Rubenstein, *The Cross-entropy Method*. New York: Springer, 2004, pp. 29-121.

[36] A. G. Asuero, A. Sayago, and A. G. González, "The correlation coefficient: an overview," *Critical Reviews in Analytical Chemistry*, vol. 36,

no. 1, pp. 41-59, Jan. 2006.
[37] R. Christie. (1993, Aug.). 118 bus power flow test case. [Online]. Available: https://www.semanticscholar.org/paper/118-Bus-Power-Flow-Test-Case-Christie/bb5529af0519cefc7e24e7b068282647c46aaed9

Gustavo Gonçalves dos Santos received the B.Sc. and M.Sc. degrees in electrical engineering from the Federal University of Uberlândia, Uberlândia, Brazil, in 2016 and 2018, respectively, and the Ph.D. degree in electrical engineering from the São Carlos School of Engineering, University of São Paulo, São Carlos, Brazil, in 2023. During his Ph.D., he was a Visiting Student at the University of Toronto, Toronto, Canada, for eight months between 2021 and 2022. From 2023 to 2024, he was a Postdoctoral Researcher in University of São Paulo. His research interests include power system voltage stability analysis, fault location, and power quality analysis, with a particular focus on harmonic distortion.

Matheus Rosa Nascimento received the B.Sc. degree in electrical engineering from the University of São Paulo, São Carlos, Brazil, in 2023. He is currently a Research Analyst at the Brazilian Energy Research Company (EPE), Rio de Janeiro, Brazil, and an M.Sc. Candidate in electrical engineering at the São Carlos School of Engineering, University of São Paulo. His research interests include dynamic security and stability of power systems.

João Pedro Peters Barbosa received the B.Sc. and M.Sc. degrees in electrical engineering from Federal University of Juiz de Fora, Juiz de Fora, Brazil, in 2021 and 2023, respectively. He is currently a D.Sc. candidate in electrical engineering at the São Carlos School of Engineering, University of São Paulo, São Carlos, Brazil. His research interests include power system stability analysis and control.

Maiara Camila Oliveira received the B.Sc. degree in electrical engineering from the Federal University of Ouro Preto, João Monlevade, Brazil, and the M.Sc. degree in electrical engineering from the University of São Paulo, São Carlos, Brazil, in 2018 and 2020, respectively. She is currently a Power System Engineer at the Brazilian TSO (Brazilian National System Operator), Rio de Janeiro, Brazil, and a Ph.D. Candidate in electrical engineering at the São Carlos School of Engineering, University of São Paulo. Her research interests include renewable energy, and power system stability analysis and control.

Ahda Pionkoski Grilo Pavani received the Ph.D. degree in electrical engineering from the University of Campinas, Campinas, Brazil, in 2008. She was a Visiting Scholar at the University of Alberta, Edmonton, Canada, in 2013, and a Visiting Professor at the Polytechnique Montreal, Montreal, Canada, from 2023 to 2024. Currently, she is a Full Professor at the Federal University of ABC - UFABC, Santo André, Brazil. Her main research interests include power system stability and control, integration of wind and PV power plants into power systems, and smart grid.

Rodrigo Andrade Ramos received the M.Sc. and Ph.D. degrees in electrical engineering from the University of São Paulo, São Carlos, Brazil, in 1999 and 2002, respectively. He is currently an Assistant Professor with the São Carlos School of Engineering, University of São Paulo. He also held positions as Visiting Associate Professor with the University of Waterloo, Warteloo, Canada, in 2013, and as a Visiting Fellow with the University of New South Wales, Canberra, Australia, in 2008. His research interests include power system stability analysis and control, with emphasis on small-signal and voltage stability problems.